A TRANSIENT PRESSURE ANALYSIS FOR WELLBORE STRENGTHENING

Yang Liu[1, 2, 3], Ping Chen[1], Tianshou Ma[1], Bisheng Wu[4], Xi Zhang[3], Bailin Wu[3]

[1]State Key Laboratory of Oil & Gas Reservoir Geology and Exploitation, Southwest Petroleum University, Chengdu, Sichuan, China

[2]Department of Mechanical Engineering, The University of Melbourne, Melbourne, Australia

[3]CSIRO Energy, Melbourne, Australia

4 Department of Hydraulic Engineering, Tsinghua University, Beijing, China

ABSTRACT

Wellbore strengthening treatments have been widely applied to improve formation bearing capacity and to mitigate lost circulation during drilling fractured formations with narrow mud-weight window. However, the mechanisms and mechanics of wellbore strengthening are still not completely understood since the fluid-solid coupling process between plugging zone and drilling fluid is previously simplified. In this paper, a fully coupled numerical model that includes rock elastic deformation, fluid flow and plugging mechanics is employed to study the evolution of plugged fracture system after wellbore strengthening. The numerical result is in good agreement with the published ones, verifying the accuracy of the present model. Symmetric bi-wing fracture geometry is considered to investigate the near-wellbore stress distribution and internal pressure profile in fracture before and after wellbore strengthening. The numerical results indicate that the hoop stress can be enhanced in compression after plugging the fractures. The evolution of fracture opening and internal pressure in fracture suggest that wellbore strengthening treatment can prolong the time to reach the fracture growth state. The existence of the plugging zone can also significantly change the normal stress distribution. In addition, the impact of plugging zone permeability on its shear failure pattern is analysed, and the relations of wellbore pressure and plugging zone failure time to the controlling parameters are discussed in detail. The limitations of the present model are also pointed out.

1 INTRODUCTION

Lost circulation is one of the most costly drilling problems encountered during drilling and a major contributor of non-productive time (NPT) (Wang et al., 2009; Shahri et al., 2014; Feng et al., 2015). According to statistics, economic losses caused by lost circulation were assessed at 2 to 4 billion dollars annually (Cook et al., 2011). However, drilling through narrow mud weight window formations, such as naturally fractured formation, pressure depleted zones, and highly pressured deep-water reservoir, may be frequently encountered, which can easily induce fractures and cause severe lost circulation (Feng and Gray, 2016; Zhong et al., 2018). Furthermore, due to drilling fluid loss, the wellbore pressure will be decreased, and consequently, it could lead to the induced wellbore collapse, induced blowout, induced pipe-sticking (Feng and Gray, 2016; Ma et al., 2017). Thus, it is necessary to take effective measures to mitigate the risk of lost circulation during drilling.

Wellbore strengthening, as an effective method to control lost circulation, is implemented by bridging and plugging fractures with multi-particles lost circulation materials (LCM) to artificially enhance the fracture pressure gradient or the formation bearing capacity. Depending on the different implementations, the main types of wellbore strengthening methods include: Stress Cage (Alberty and McLean, 2004), Fracture Closure Stress (Dupriest, 2005) and Fracture Propagation Resistance (van Oort et al., 2011). A large number of lab experiments and successful field applications have demonstrated the feasibility and practicability of wellbore strengthening (Onyia, 1994; Guo et al., 2014; Xu et al., 2017), but the filed treatment results are of high randomness. Several studies adopted numerical simulation method to reveal the mechanisms and the mechanics of wellbore strengthening, and got fairly consistent results on wellbore strengthening effects. Alberty and McLean (2004), and Feng et al. (2015) investigated the evolution of hoop stress during wellbore strengthening and conducted a comprehensive parametric analysis based on finite-element analyses. Wang et al. (2007, 2009) developed a 2D boundary-element model to study the fracture opening, tangential stress change, and fracture growth stability for stress cage treatment under anisotropic in-situ stress conditions. The numerical results indicated that the hoop stress can be significantly improved after plugging the fractures, and the increasing magnitude is strongly influenced by in-situ stress and plugging geometrical parameters. However, there still exist various extents of shortcomings due to some simplified assumptions. For instance, the assumption of fixed pressure boundary may underestimate or overestimate the fracture pressure, and some models have not taken into account the influence of fluid flow. Hence, these models cannot give the variation of internal pressure in fracture during wellbore strengthening.

For this purpose, this paper develop a fully coupled numerical model, which includes rock elastic deformation, fluid flow and plugging geometrical parameters, to further investigate wellbore strengthening effect. The simulation result is validated with the published ones. Subsequently, this study compares the near-wellbore stress, fracture opening, internal pressure and normal confining stress before and after wellbore strengthening. The impact of plugging zone permeability on its shear failure pattern is analysed, and the relations of wellbore pressure and plugging zone failure time to the controlling parameters are discussed in detail. The limitations of the present model are also pointed out.

2 MODEL

Figure 1 illustrates the problem of wellbore strengthening for a well in an impermeable formation characterized by Young's modulus *E*, Poisson's ratio *v* and fracture toughness K_{IC}. Two fractures emanating from wellbore are considered symmetric and their surfaces coincide with the maximum horizontal stress (σ_{H}) or *x*-axial direction. The near wellbore stress analysis can be represented by a plane strain condition preassembly. Due to the existence of multi-particle LCM in the drilling fluid, the pre-existing wellbore fractures can be bridged and plugged during drilling fluid circulation, as shown in Fig.1. The LCM plugged zone is assumed to have certain permeability and the permeability can be adjusted by optimizing the selection of LCM type and concentration. The fluid leaking off into the formation can be ignored in a low-permeability shale gas reservoir. The initial fracture length and fracture conductivity are characterized by *L* and w_0, respectively. The shape of plugging zone is assumed to be rectangle and characterized by *b* (length) and w_p (width), and the width of plugging zone is the same as the initial conductivity wellbore fracture.

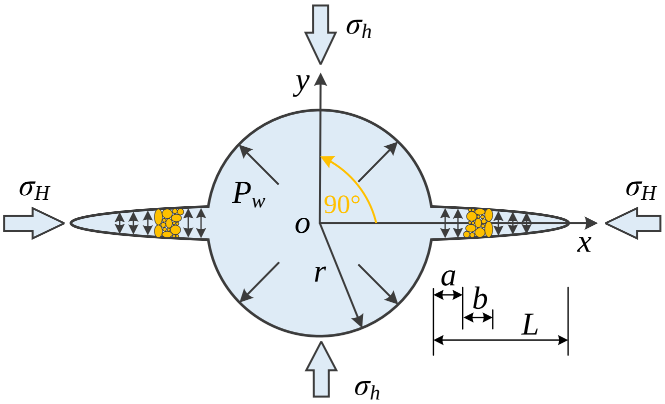

Figure 1: Mechanical model of two symmetric fractures plugged with LCM

2.1 ELASTICITY

For the fracture system as shown in Fig.1, the elasticity equilibrium equation can be expressed by the displacement discontinuities (DDs) formulation (Hills et al., 1996; Zhang et al., 2005), in the form of,

$$P_f(\boldsymbol{x},t)-\sigma_n(\boldsymbol{x})=\int_\Sigma [G_{11}(\boldsymbol{x},s)w(s)+G_{12}(\boldsymbol{x},s)v(s)]\,ds \tag{1}$$

$$0=\int_\Sigma [G_{21}(\boldsymbol{x},s)w(s)+G_{22}(\boldsymbol{x},s)v(s)]\,ds \tag{2}$$

where $\boldsymbol{x}=(x,t)$ and *t* is time; *ds* is the infinitesimal path length along the fracture; *w* and *v* are mechanical opening and relative sliding (normal and shear displacement discontinuities) along fracture surfaces. P_f is the pressure of the fluid-filled parts of the fracture. σ_{n} is the normal stress components generated by the far-field stresses. The integration contour Σ is the union of the crack and the circular wellbore wall. G_{ij} are hyper singular Green's functions (Zhang et al., 2007).

When the fractures are absent, the normal stress acting on the x axis can be determined by Kirsch solution,

$$\sigma_n(\boldsymbol{x})=\sigma_h\left(1+\frac{r^2}{x^2}\right)+\frac{\sigma_H-\sigma_h}{2}\left(\frac{r^2}{x^2}-3\frac{r^4}{x^4}\right)-P_w\frac{r^2}{x^2} \tag{3}$$

2.2 FLUID FLOW

Considering the laminar flow of an incompressible Newtonian fluid in the fracture, the fluid flux q can be described by Poiseuille law (Batchelor, 1967),

$$q = -\frac{(w+\varpi)^3}{\mu'}\ \frac{\partial P_f}{\partial s} \tag{4}$$

where $\mu' = 12\mu$ and μ denotes dynamic viscosity and ϖ is the hydraulic aperture that does not contribute to stress change. According to fluid mass balance, the local continuity equation can be expressed as,

$$\frac{\partial(w+\varpi)}{\partial t} + \frac{\partial q}{\partial s} = 0 \tag{5}$$

Substituting Eq. (4) into Eq. (5), the Reynolds' lubrication equation can be deduced to describe fluid flow movement inside the opened fractures,

$$\frac{\partial w}{\partial t} = \frac{\partial}{\partial s}\left[\frac{(w+\varpi)^3}{\mu'}\ \frac{\partial P_f}{\partial s}\right] \tag{6}$$

For plugged zone, the fluid flow can be described by the following pressure diffusion equation (Zhang et al., 2009, 2011),

$$\frac{\partial P_f}{\partial t} = \frac{1}{\kappa\mu'}\frac{\partial}{\partial s}\left(\varpi^2\ \frac{\partial P_f}{\partial s}\right) \tag{7}$$

where κ is called as the fracture compressibility to highlight the fracture dilation as pressure decreases.

2.3 AUXILIARY CONDITIONS AND FAILURE CRITERION

The initial and boundary conditions are required to solve the above governing equations. At the fracture tip, the opening, shearing DDs and fluid flux are identically equal zero, namely,

$$w(L,t) = v(L,t) = 0 \tag{8}$$

$$q(L,t) = 0 \tag{9}$$

Additionally, the borehole pressure is set equal along the inner wall of the wellbore and keeps constant in this paper. The fluid pressure at the fracture mouth should satisfy the following equations,

$$P_f(0,t) = P_w \tag{10}$$

Fracture propagation occurs when the crack-tip stress intensity factors (SIFs) exceed the fracture toughness of rock. The fracture propagation direction can be calculated by using the mixed-mode failure criterion proposed by Erdogan and Sih (1963). Considering mixed-mode crack growth, the mixed SIFs at the fracture tip can be obtained by the displacement correlation method (Zhang et al., 2005), and if fracture deflection is involved, the fracture propagation direction is determined by solving the following equation,

$$K_I \sin\vartheta + K_{II}(3\cos\vartheta - 1) = 0 \tag{11}$$

where ϑ is the deflection angle from the current fracture line. K_I and K_{II} are the Mode I and Mode II SIFs, respectively. The stress intensity factors must meet the following condition at the onset of crack growth (Erdogan and Sih, 1963),

$$\cos\frac{\vartheta}{2}\left(K_I\cos^2\frac{\vartheta}{2} - \frac{3}{2}K_{II}\sin\vartheta\right) = K_{IC} \tag{12}$$

where K_{IC} is the tensile fracture toughness.

3 MODEL VALIDATION

The main purpose of this paper is to analyse the near-wellbore stress distribution and internal pressure profile in fracture during wellbore strengthening by particle plugging. The numerical results, developed by Wang et al. (2009), are first selected to verify the accuracy of the proposed model. The model they used for solving elasticity equation is also based on boundary-element method as we developed (Zhang et al, 2005, 2007, 2009). For the coupled problems, we used finite volume method to solve the fluid flow equation. In particular, the two equations are solved by an iteration method so that the targeted solutions of fracture deformation and internal pressure are within a given tolerance.

The modelling geometry for verification is shown in Fig.2, with the fracture is plugged at the mouth. A fracture emanating from wellbore wall is 0.15 m long. The wellbore pressure is specified as 27.6 MPa, the internal pressure in fracture (P_f) is assumed to be equal to the minimum horizontal stress (σ_h=20.7 MPa), and the maximum horizontal stress is 41.4 MPa. We use exactly the same values of input parameters that can be found in Wang et al. (2009).

Figure 3 displays the comparison of fracture opening after plugging the fracture with LCM. It shows that our result is in agreement with the previous one in Wang et al. (2009), verifying the accuracy of the present model in solving an elastic problem. In addition, it should be pointed out that the previous boundary-element model uses a constant internal pressure in fracture, which may be inconsistent with real situation. In our model, the internal pressure in fracture is calculated by the lubrication equation or pressure diffusion equation and is closely related to the wellbore pressure. Therefore, the proposed model is suitable to transiently track the pressure variation along the fracture.

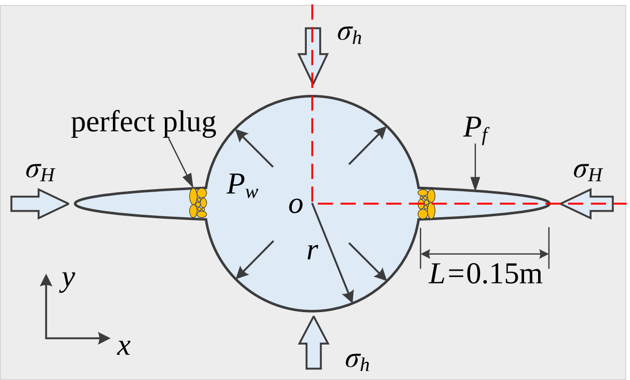

Figure 2: The geometry and boundary conditions of the wellbore strengthening model

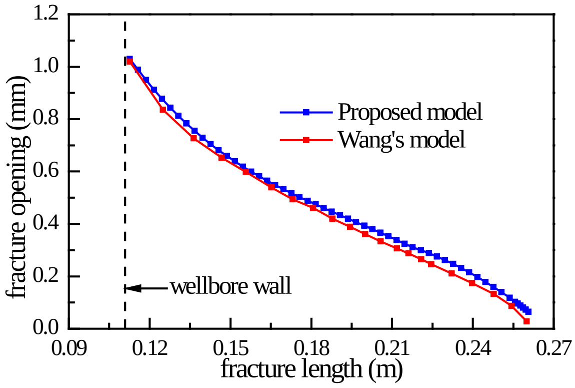

Figure 3: Comparison of fracture opening between two methods after plugging the fracture with LCM

4 NUMERICAL RESULTS

4.1 MODELING PARAMETERS DETERMINATION

The correct choice of wellbore pressure and mechanical parameters is of greatest importance for wellbore strengthening analysis under constant wellbore pressure condition. Here, the parameters for the Longmaxi Formation of Well JY-1 in Sichuan Basin are used as the basic parameters (Wang and Sun, 2015). The Longmaxi Formation belongs to the typical shale formation. The logging data indicate that the Longmaxi Formation has the vertical stress gradient of 2.44 MPa/100m, the maximum horizontal stress gradient of 2.65 MPa/100m, the minimum horizontal stress gradient of 1.96 MPa/100m at the depth of 2400 m. The measured pore pressure, collapse pressure and breakdown pressure profiles, represented by equivalent mud density, are depicted in Fig.4. One thing should be mentioned that the calculated pore pressure gradient after hydraulic fracturing is about 1.55 g/cm^3.

This vertical well was drilled successfully by using OBM with the density of 1.70~1.77 g/cm^3. No serious wellbore instability and drilling fluid leakage were reported. In order to compare the stability of fracture system in the presence and absence of wellbore strengthening, the wellbore pressure is specified as 47.5 MPa. The reason for using this pressure level is that it can propagate the pre-existing fractures so that the wellbore strengthening is necessary. Since the Longmaxi Formation is of low permeability, the reservoir pressure is not changed too much during drilling and can be taken out of the stress levels and wellbore pressure. In particular, it is assumed to be zero in the calculations.

Besides, the mechanical parameters of Longmaxi shale are measured experimentally by using seven samples, as shown in Fig.5. All our simulations are conducted with a Young’s modulus of 38 GPa, a Poisson's ratio of 0.22, and a fracture toughness of 1.0 MPa · m$^{0.5}$. These constants can be treated as the averages of seven samples. The permeability of plugging zone is set as 0.5 Darcy. Other parameters used in the simulations are listed in Table 1.

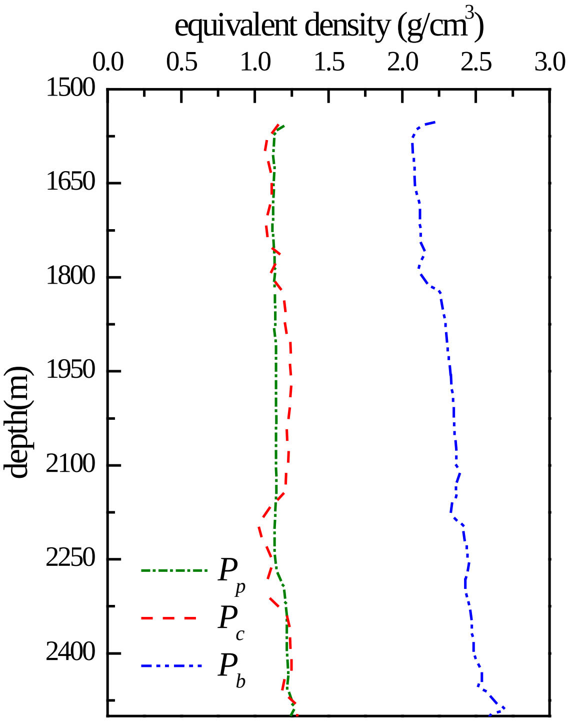

Figure 4: The predicted pressure profile of Well JY-1 (Wang and Sun, 2015). Here P_p is pore pressure, P_c is collapse pressure and P_b is breakdown pressure.

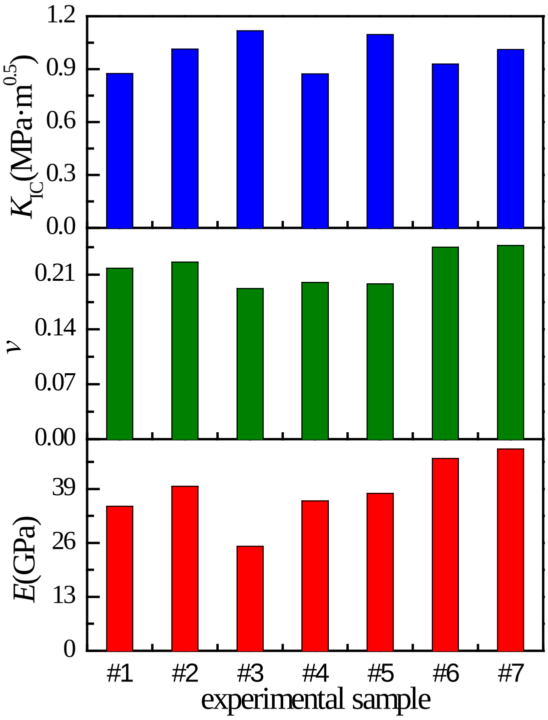

Figure 5: The experimental results of mechanical parameters at the Longmaxi Formation of Well JY-1.

4.2 GENERAL FEATURES

Cases A and B are used to compare the effect of wellbore strengthening treatment on fracture system stability. Figure 6 (a) shows the hoop stress on the wellbore wall before and after wellbore strengthening. The hoop stress around the wellbore wall is determined at the distance of 0.105 m to the borehole centre. We use the sign conversation with the negative values for compressive stresses throughout this paper. Obviously, the hoop stress on the wellbore wall always is in compression and can be enhanced after plugging the fractures because the hoop stress can be increased in compression. The maximum increase is about 2.0 MPa. It is generally used as the measure of wellbore strengthening. However, it evolves with the changes in wellbore pressure and the time-dependent increase of internal pressure in fracture. Actually, the wellbore strengthening effect can also be improved by decreasing the permeability of plugging zone. This is due to the fact that the lower the permeability of plugging zone, the stronger the blockage of fluid flow in increasing the internal pressure. This further implies that the transient pressure analysis is important to assess the final results of wellbore strengthening by LCM plugging method.

Figures 6 (b) and (c) show the evolution of fracture opening and internal pressure in fracture before and after wellbore strengthening. It is shown that the fracture opening close to crack-tip is closed at the early stage because the internal pressure in this region is less than the minimum horizontal stress. Near the fracture mouth, the opening and internal pressure of plugged fracture are larger than those of the unplugged fracture. This is because after plugging the fracture, the pressure diffusion along the fracture length can be restricted. Later the internal pressure in fracture will accumulate to the level so that the plugging zone is fully opened. In the end, the fracture opening and internal pressure with and without plugging are slightly different as displayed in Figs. 6(b) and (c). However, in the presence of plugging, the time to reach the final state is prolonged. In reality, the pressure is maintained by constantly injecting drilling fluid into the well. This slight postponing for fractures to initiate can provide more warning time in reducing the wellbore pressure by decreasing the injection rate. In other words, this transient pressure analysis can provide the minimum wellbore pressure that can generate fracture growth when the LCM plugging is permeable.

Besides, the normal confining stress, defined as the sum of internal pressure and contact stress on plugging zone and fracture surface, reflect the difficulty in opening up the plugging, or the success of wellbore strengthening (Fig.6 (d)). After plugging the fracture, the existence of the plugging zone can significantly change the normal stress distribution. The normal stress normally on the plugging zone is increased much and this stress can impede fluid penetration across the plugging zone, as shown in Fig. 6(d). Moreover, the stress ahead the plugging zone can be reduced. This fracture portion may be opened by the presence of the plugging zone and can play a role as the storage of the fluid penetrating the plugging zone. The filling of this fracture portion is progressive and it can assist the failure of the plugging zone and the fracture growth from the crack tip. Therefore, the transient pressure analysis becomes important mainly because the steady-state results may overestimate the maximum wellbore pressure that the wellbore strengthening effect can afford.

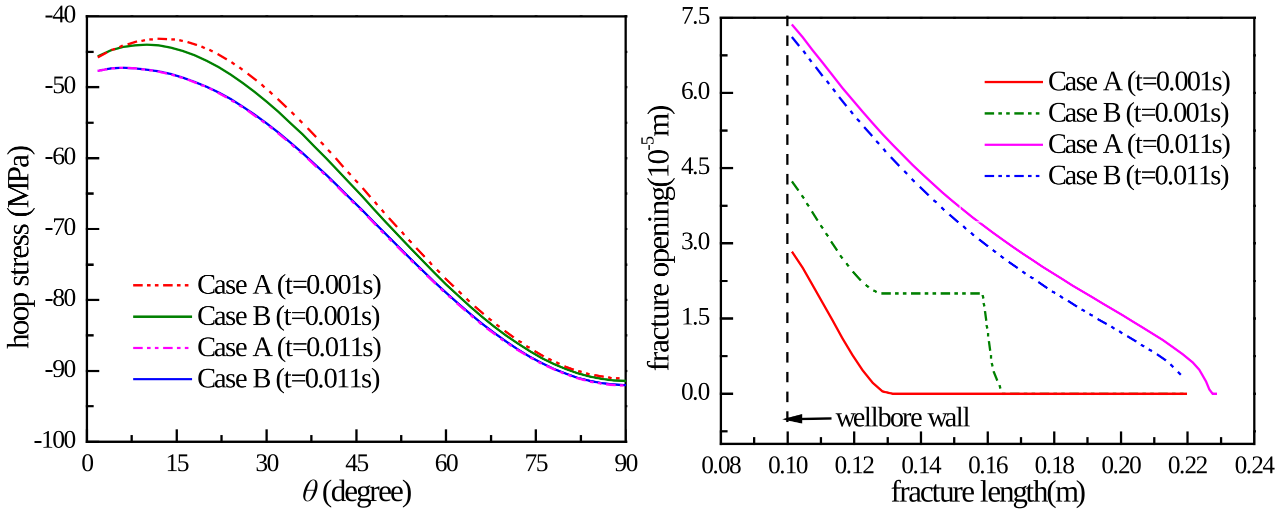

(a) Hoop stress **(b) Fracture opening**

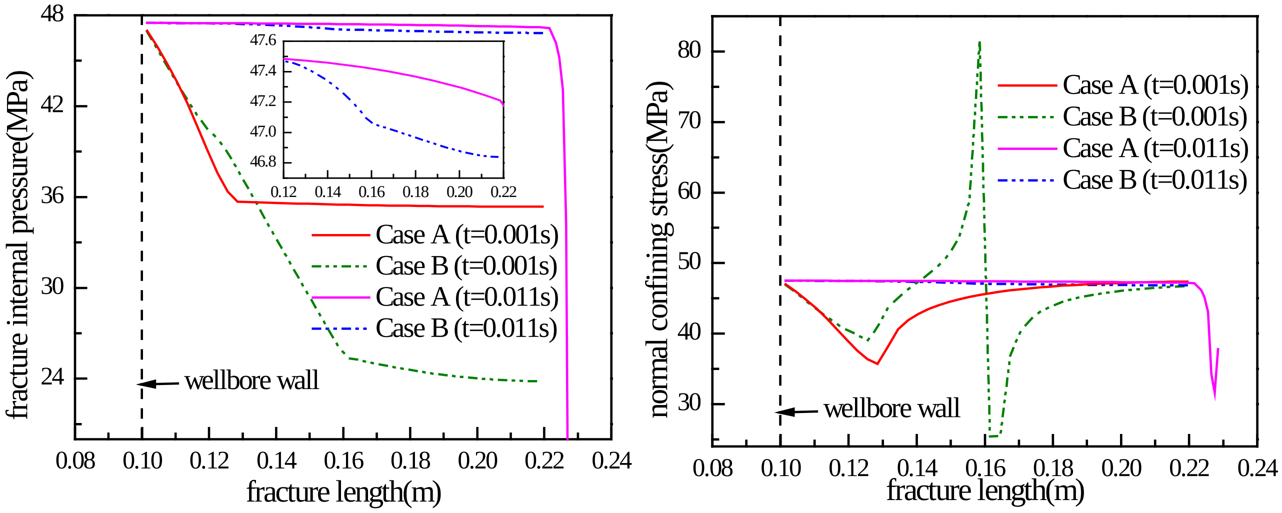

(c) Fracture pressure **(d) Normal confining stress**

Figure 6: Variation of parameters for fracture system before and after wellbore strengthening. Cases A and B represent the unplugged and plugged fracture, respectively.

5 DISCUSSION

5.1 PERMEABILITY OF PLUGGING ZONE

The previous investigations indicate that the failure of the plugging zone can be caused by frictional failure and shear failure (Xu, 2015; Xu et al., 2017). The frictional failure refers to that the plugging zone slips as a whole and this can be caused by the increase in fracture opening. The shear failure means that some part of the plugging zone breaks and leaves a conduit for fluid to flow towards the crack tip. The former is related to the critical opening in overcoming the barrier and the latter to the shear strength of the plugging zone. The shear failure is more likely to occur during wellbore strengthening (Xu, 2015). The various failure modes of the plugging zone are displayed in Fig. 7.

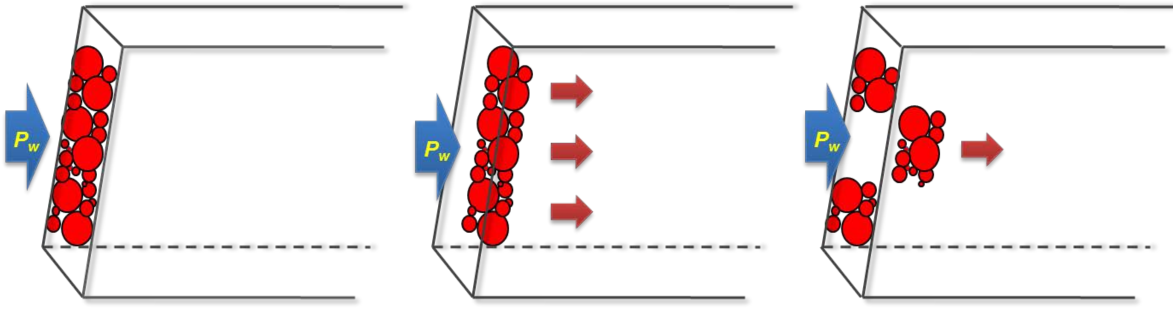

(a) Stable plugging zone **(b) frictional failure patterns** **(c) shear failure patterns**

Figure 7: Schematic of fracture-plugging zone and its two typical failure patterns (Xu et al. 2017)

To represent the wellbore strengthening effect, the wellbore strengthening index (WSI) is introduced to describe the desired amount of strengthening (Chellappah et al., 2018),

$$WSI = \left(\frac{(P_w - \sigma_h)}{E'} + \alpha \frac{(\sigma_H - \sigma_h)}{E'}\right) \times 1000 \tag{13}$$

Where P_w is the target wellbore pressure; E' is plain-strain elastic modulus, $E' = E/(1-\upsilon^2)$; υ is the Poisson's ratio. α is a weighting factor for stress anisotropy and it is set as a default value of 0.25. Clearly, the index is directly proportional to the wellbore pressure for a given in-situ stress situation. It also illustrates that the wellbore strengthening has no effect unless the WSI is greater than zero. This criterion can be used to determine the lower bound of target wellbore pressure during wellbore strengthening, namely, $P_{wl} = 1.25\sigma_h - 0.25\sigma_H$.

It should be mentioned that the pressure difference is not a constant in the presence of a permeable plugging zone. The fluid can pass through the plugging zone and enhance the pressure at the downstream of the plugging zone. This can alleviate the pressure difference and reduce the risk for the shear failure of the plugging zone. The variations of pressure difference on the two sides of the plugging zone versus plugging zone permeability are displayed in Fig.8. The wellbore pressure is specified as 46.0 MPa to prevent the failure of plugging zone caused by the increase of fracture opening, and the corresponding WSI is about 0.08. The shear strength of the plugging zone can be calculated by using the published model and the material parameters of the plugging zone are the same as those used by (Xu et al., 2017). It can be clearly noted that the risk for the shear failure of the plugging zone may grow with the decrease of plugging zone permeability. The results reveal that besides the LCM type and concentration, the permeability of plugging zone may also need to be optimized for maximum wellbore strengthening effect.

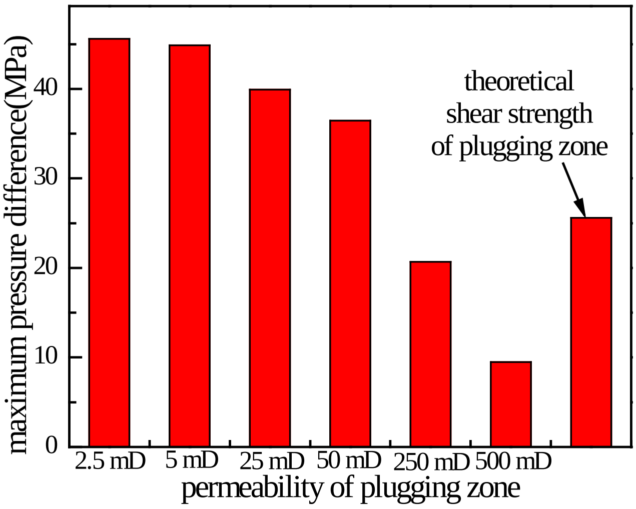

Figure 8: The relations of the plugging zone failure time with its permeability.

For high-permeable plugging zone, the relations of the plugging zone failure time and WSI with wellbore pressure are shown in Fig.9. At this time, the failure of plugging zone is mainly caused by the increase of fracture opening. The permeability of plugging zone is set as 0.5 Darcy to avoid the shear failure of plugging zone. It can be found that the dimensionless failure time decreases nonlinearly with wellbore pressure, while the WSI increases linearly with wellbore pressure. When the wellbore pressure exceeds the minimum horizontal principle stress, the plugging zone loses its stability rapidly; when wellbore pressure is lower than the minimum horizontal principle stress, the stability of plugging zone increases sharply with the declining of wellbore pressure. This means that the transient pressure analysis is critical in preventing the failure of the plugging zone and the steady-state solution has overestimated this risk.

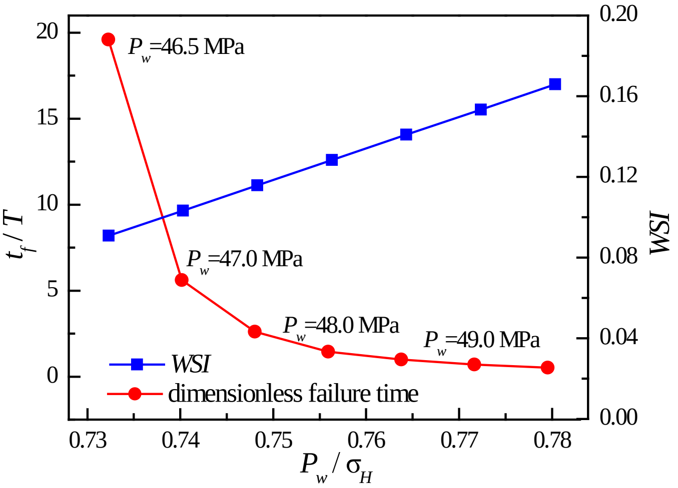

Figure 9: The relations of the plugging zone failure time and WSI with wellbore pressure. The plugging zone failure time and wellbore pressure are transformed to the dimensionless form by using $T\left(T = \left(\frac{\mu' L^6}{E' Q_0^3}\right)^{1/4}\right)$ and σ_H.

5.2 MODELING LIMITATIONS AND FURTURE WORK

The model developed here is based on the constant wellbore pressure. In fact, the addition of drilling fluid into the wellbore is performed at a constant injection rate and the wellbore pressure oscillates within a narrow range. The wellbore strengthening effect under a fixed injection rate is not studied here, but it is important. Although the transient pressure analysis is necessary in finding the accurate maximum wellbore pressure and the pressure difference on the two sides of the plugging zone, the critical pressure at various controlling parameters has not been explored in this paper. However, a safe mud weight window is imperative especially when the steady-state solutions currently used overestimate the wellbore pressure levels and further research is required.

6 REFERENCE

Alberty, M. W., McLean, M. R. (2004). A physical model for stress cages. SPE annual technical conference and exhibition. SPE Annual Technical Conference and Exhibition, 26-29 September, Houston, Texas. (SPE-90493-MS).

Batchelor G. K. (1967). An Introduction to Fluid Dynamics. Cambridge University Press.

Chellappah, K., Majidi, R., Aston, M., Cook, J. (2018). A Practical Model for Wellbore Strengthening. In IADC/SPE Drilling Conference and Exhibition. IADC/SPE Drilling Conference and Exhibition, 6-8 March, Fort Worth, Texas, USA. (SPE-189589-MS).

Cook, J., Growcock, F., Guo, Q., Hodder, M. and van Oort, E. (2011). Stabilizing the wellbore to prevent lost circulation. Oilfield Review, 23(4), 26-35.

Dupriest, F. E. (2005). Fracture closure stress (FCS) and lost returns practices. SPE/IADC Drilling Conference, 23-25 February, Amsterdam, Netherlands. (SPE-92192-MS).

Erdogan, F. and Sih, G.C. (1963). On the crack extension in plates under plane loading and transverse shear. Journal of basic engineering, 85(4), 519-525.

Feng, Y., Arlanoglu, C., Podnos, E., Becker, E. and Gray, K.E. (2015). Finite-element studies of hoop-stress enhancement for wellbore strengthening. SPE Drilling & Completion, 30(01), 38-51. (SPE-168001-PA).

Feng, Y., Gray, K. E. (2016). A parametric study for wellbore strengthening. Journal of Natural Gas Science and Engineering, 30, 350-363.

Guo, Q., Cook, J., Way, P., Ji, L., Friedheim, J. E. (2014). A comprehensive experimental study on wellbore strengthening. IADC/SPE drilling conference and exhibition. IADC/SPE Drilling Conference and Exhibition, 4-6 March, Fort Worth, Texas, USA. (SPE-167957-MS).

Hills, D. A., Kelly, P. A., Dai, D. N., Korsunsky, A. M., Keer, L. M. 1996. Solution of crack problems: the distributed dislocation technique. Solid mechanics and its applications, vol. 44. Dordrecht: Kluwer Academic Publishers.

Kirsch G. (1898). Die Theorie der Elastizität und die Bedürfnisse der Festigkeitslehre. Springer.

Ma, T., Wu, B., Fu, J., Zhang, Q., Chen, P. (2017). Fracture pressure prediction for layered formations with anisotropic rock strengths. Journal of Natural Gas Science and Engineering, 38, 485-503.

Onyia, E. C. (1994). Experimental data analysis of lost-circulation problems during drilling with oil-based mud. SPE Drilling & Completion, 9(01), 25-31. (SPE-22581-PA)

Shahri, M.P., Oar, T., Safari, R., Karimi, M. and Mutlu, U. (2014). Advanced geomechanical analysis of wellbore strengthening for depleted reservoir drilling applications. IADC/SPE Drilling Conference and Exhibition, 4-6 March, Fort Worth, Texas, USA. (SPE-167976-MS).

Van Oort, E., Friedheim, J. E., Pierce, T., Lee, J. (2011). Avoiding losses in depleted and weak zones by constantly strengthening wellbores. SPE Drilling & Completion, 26(04), 519-530.

Wang, H., Soliman, M.Y. and Towler, B.F. (2009). Investigation of factors for strengthening a wellbore by propping fractures. SPE Drilling & Completion. 24, 441-451. (SPE-112629-PA).

Wang, H., Towler, B. F., Soliman, M. Y. (2007). Fractured wellbore stress analysis: sealing cracks to strengthen a wellbore. SPE/IADC Drilling Conference, 20-22 February, Amsterdam, Netherlands. (SPE-104947-MS).

Wang, Z.G., Sun, J. (2015). Practice and Cognition of Well-groups Development in Fuling Shale Gas Field. China Petrochemical Press.

Xu, C. (2015) Models and methods to strengthen wellbore pressure containment by fracture plugging in fractured reservoirs. Southwest Petroleum University. (PhD dissertation).

Xu, C., Kang, Y., You, L., You, Z. (2017). Lost-circulation control for formation-damage prevention in naturally fractured reservoir: mathematical model and experimental study. SPE Journal, 22(05), 1-654.

Zhang, X., Jeffrey, R.G., Detournay, E. (2005). Propagation of a hydraulic fracture parallel to a free surface. International journal for numerical and analytical methods in geomechanics, 29(13), 1317-1340.

Zhang, X., Jeffrey, R. G., & Thiercelin, M. (2007). Deflection and propagation of fluid-driven fractures at frictional bedding interfaces: a numerical investigation. Journal of Structural Geology, 29(3), 396-410.

Zhang, X., Jeffrey, R. G. and Thiercelin, M. (2009). Mechanics of fluid‐driven fracture growth in naturally fractured reservoirs with simple network geometries. Journal of Geophysical Research: Solid Earth, 114(B12).

Zhang, X., Jeffrey, R. G., Bunger, A. P., Thiercelin, M. (2011). Initiation and growth of a hydraulic fracture from a circular wellbore. International Journal of Rock Mechanics and Mining Sciences, 48(6), 984-995.

Zhong, R., Miska, S., Yu, M., Ozbayoglu, E., & Takach, N. (2018). An integrated fluid flow and fracture mechanics model for wellbore strengthening. Journal of Petroleum Science and Engineering, 167, 702-715.